BJP BRITISH JOURNAL OF PHARMACOLOGY
BPS BRITISH PHARMACOLOGICAL SOCIETY

BJP British Journal of Pharmacology

DOI:10.1111/j.1476-5381.2010.01025.x
www.brjpharmacol.org

RESEARCH PAPER

Receptor localization, native tissue binding and *ex vivo* occupancy for centrally penetrant P2X7 antagonists in the rat

SL Able, RL Fish, H Bye*, L Booth, YR Logan, C Nathaniel, P Hayter and SD Katugampola

Pfizer Global Research and Development, Sandwich, UK

Correspondence
SL Able, New Opportunities Unit, Pfizer Global Research and Development, Ramsgate Road, Sandwich, Kent CT13 9NJ, UK.
E-mail: sarah.able@pfizer.com

*Present address: Kings College, London, UK.

Keywords
P2X7 receptor; rat cortex; radioligand binding; occupancy

Received
4 May 2010
Revised
26 July 2010
Accepted
24 August 2010

BACKGROUND AND PURPOSE
The P2X7 receptor is implicated in inflammation and pain and is therefore a potential target for therapeutic intervention. Here, the development of a native tissue radioligand binding, localization and *ex vivo* occupancy assay for centrally penetrant P2X7 receptor antagonists is described.

EXPERIMENTAL APPROACH
Autoradiography studies using the P2X7 antagonist radioligand [^{3}H]-A-804598 were carried out in rat brain and spinal cord. Subsequent *in vitro* binding and *ex vivo* occupancy assays were performed using rat cortex homogenate.

KEY RESULTS
P2X7 expression was shown to be widespread throughout the rat brain, and in the grey matter of the spinal cord. In binding assays in rat cortex homogenate, ~60% specific binding was achieved at equilibrium. In kinetic binding assays, k_{on} and k_{off} values of 0.0021·min^{-1}·nM^{-1} and 0.0070·min^{-1} were determined, and the K_d derived from kinetic measurements was consistent with that derived from saturation analysis. Novel P2X7 antagonists inhibited the binding of [^{3}H]-A-804598 to rat cortex P2X7 receptors with K_i values of <40 nM. In an *ex vivo* occupancy assay, a P2X7 antagonist dosed orally to rats caused a concentration-dependent inhibition of the specific binding of [^{3}H]-A-804598 to rat cortex.

CONCLUSIONS AND IMPLICATIONS
The present study describes the development of an assay that allows localization of P2X7 receptors, the measurement of the binding affinity of P2X7 receptor antagonists in native tissue, and provides a means of determining central P2X7 receptor occupancy. These assays could form an important part of a P2X7 drug discovery programme.

Abbreviations
BSA, bovine serum albumin; BZ-ATP, 2′3′-O-(4-benzoylbenzoyl)adenosine 5-triphosphate; DMSO, dimethyl sulphoxide; FLIPR, fluorometric imaging plate reader; L4–L6, lumbar vertebrae in the rat spinal cord

Introduction

The P2X7 receptor is a member of the P2X family of ATP-gated ion channels. It differs from other P2X family members in that it is functional only in homomeric forms, and it is activated only by high concentrations of ATP (North, 2002). Brief exposure of the receptor to agonists results in elevated intracellular calcium due to the opening of cation channels, whereas prolonged exposure results in the

formation of a non-selective pore, allowing the influx of larger cations as well as large hydrophilic molecules (Ferrari *et al.*, 1996; Rassendren *et al.*, 1997). The P2X7 receptor was cloned initially from rat (Surprenant *et al.*, 1996), and the human and mouse receptors were subsequently cloned and shown to have around 80% homology with the rat receptor (Rassendren *et al.*, 1997; Chessell *et al.*, 1998).

Northern blotting studies showed a widespread tissue distribution of P2X7 mRNA throughout the rat immune system and also in other organs such as brain, spinal cord, skeletal muscle, lung and placenta (Collo *et al.*, 1997; Rassendren *et al.*, 1997). In the central nervous system (CNS), expression of the receptor on astrocytes, microglial cells and neurones has been demonstrated using immunohistochemical methods (Deuchars *et al.*, 2001; Kukley *et al.*, 2001; Xiang and Burnstock, 2005). However, the specificity of some commercially available P2X7 antibodies has been called into question by researchers who demonstrated staining in tissues from P2X7 knock-out mice (Sim *et al.*, 2004; Anderson and Nedergaard, 2006). This field has now been complicated further by the discovery that knock-out animals may still express truncated splice variants of P2X7 due to incomplete inactivation of the gene (Nicke *et al.*, 2009). This confusion highlights the need to develop specific, selective and high affinity radioligands to demonstrate a clearer representation of receptor protein localization.

Activation of P2X7 receptors on cells of the immune system triggers the release of a number of cytokines and inflammatory mediators (Ferrari *et al.*, 1997; Sperlágh *et al.*, 1998; Bulanova *et al.*, 2005). In the nervous system, P2X7 receptors have been shown to play a role in the modulation of neurotransmitter release (Deuchars *et al.*, 2001; Sperlágh *et al.*, 2002), and in microglial and astroglial activation (Bianco *et al.*, 2006; Suadicani *et al.*, 2006). Hence there is therapeutic rationale for the use of P2X7 antagonists in the treatment of a variety of disease states, from inflammatory diseases such as rheumatoid arthritis, to the amelioration of neuropathic pain.

The synthesis of a radiolabelled P2X7 receptor antagonist, [^{3}H]-A-804598, was recently reported in the literature, and the binding characteristics of this ligand at rat recombinant P2X7 receptors were described (Donnelly-Roberts *et al.*, 2009). The aim of the current study was to use this ligand to investigate P2X7 receptor localization in the rat brain and spinal cord, and to develop a rat native tissue P2X7 homogenate binding assay. In addition, the suitability of the homogenate binding assay methodology to measure *ex vivo* occupancy of dosed P2X7 receptor antagonists was investigated, in order to provide a means of demonstrating target engagement of centrally penetrant P2X7 receptor antagonists.

Methods

Animals and tissue collection

Male Sprague-Dawley rats (200–300 g), purchased from Charles River Laboratories (UK) were kept in a fixed 12 h light–dark cycle with food and water provided *ad libitum*. Rats were culled by decapitation and tissues were removed and frozen on isopentane cooled to –40°C on dry ice. All experiments were conducted in compliance with the Home Office Guidance on the operation of the Animals (Scientific Procedures) Act (1986) under the authority granted in personal and project licenses, and were reviewed and approved by the ethical review panel.

Fluorometric imaging plate reader (FLIPR) assay

A FLIPR assay was used to confirm the functional potency of A-804598 and two other novel P2X7 antagonists; Compound A (Nelson *et al.*, 2006) and A-740003 (Honore *et al.*, 2006). rP2X7-1321N1 cells (cells expressing the rat recombinant P2X7 receptor) were maintained in a humidified 37°C incubator under 5% CO_2. The culture media was MEM Alpha containing 10% dialysed foetal bovine serum, 100 U·mL^{-1} penicillin G sodium, 100 µg·mL^{-1} streptomycin sulphate and 350 µg·mL^{-1} geneticin. The cells were plated at 2×10^5 cells·mL^{-1} into 384-well poly-D-lysine coated black/clear bottom plates. The plates were incubated overnight in a humidified 37°C incubator under 5% CO_2.

The FLIPR Calcium 4 assay kit (Molecular Devices, Wokingham, UK) was used for these experiments. The dye supplied with the kit was resuspended in assay buffer (20 mM HEPES buffered Hank's balanced salt solution at pH 7.4). The cell plate was quickly inverted over a sink to remove the culture media and it was replaced with 25 µL per well of the buffered dye. The cells were then placed back in the incubator for 60 min and the plate then transferred to a FLIPR Tetra. The cells were pre-incubated with P2X7 antagonists (25 µL) for 10 min, and BZ-ATP (100 µM; an approximate EC_{80} concentration) was then added and the calcium influx recorded as relative fluorescence units.

In vitro *autoradiography*

Cryostat sections (20 µm) were cut coronally through a rat brain and the L4–L6 region of rat spinal cord, and thaw-mounted onto poly-L-lysine coated slides. Slides were stored at –80°C until use.

Sections were incubated for 2 h at 4°C with 5 nM [^{3}H]-A-804598 in assay buffer (50 mM Trizma/0.1% BSA, pH 7.4 at 4°C) either in the absence (total binding) or presence (non-specific binding) of 10 μM A-740003. Sections were rinsed (2 × 5 min) in ice-cold 50 mM Trizma, followed by a brief dip in distilled water, and dried under a stream of cold air. Slides were imaged using a Beta-imager (BioSpace, Paris, France) for 12 h under high resolution.

In vitro *homogenate binding*

[^{3}H]-A-804598 binding was performed in assay buffer (50 mM Trizma/0.1% BSA, pH 7.4 at 4°C) at 4°C for 2 h in a total volume of 250 μL, using 300 μg of cortex homogenate per well. Non-specific binding was defined using 10 μM A-740003. Concentration-dependent (saturation) binding was performed using 12 concentrations of [^{3}H]-A-804598 (0.5–50 nM). For association experiments, cortex homogenate was incubated with 5 nM [^{3}H]-A-804598 for intervals from 2 min to 5 h in the presence and absence of 10 μM A-740003. For dissociation experiments, cortex homogenate was incubated with 5 nM [^{3}H]-A-804598 for 2 h to allow association of [^{3}H]-A-804598. After this time an excess (10 μM) of A-740003 was added to each well at various times, and dissociation followed from 2 min to 4 h. Competition binding experiments were performed using 5 nM [^{3}H]-A-804598, an approximate K_d concentration, in the presence and absence of P2X7 antagonists. IC_{50} values were determined using 10 half-log serial dilutions in duplicate.

Binding assays were terminated by separation of bound and free radioligand by filtration through GF/B filters pre-soaked in 0.5% polyethyleneimine using a Brandel harvester. Filter circles were punched out using a Brandel punch-out machine, and counted on a Tricarb liquid scintillation counter (Perkin Elmer, Seer Green, UK).

Ex vivo *receptor occupancy studies*

Rats (four per treatment group) were orally dosed with Compound A at 3, 10, 30 and 100 mg·kg^{-1} or vehicle (0.5% methylcellulose) and subsequently killed by decapitation at 1 h post dose. Trunk blood samples were collected immediately after decapitation and the plasma was separated by centrifugation for determination of drug concentration. The cortex was removed and frozen immediately in isopentane (cooled to –40°C with dry ice) and stored at –80°C until use.

For the *ex vivo* homogenate binding assay, cortex samples were weighed and homogenized in 12 mL assay buffer·g^{-1} weight tissue (giving a protein concentration of approximately 1.75 mg per well). The binding assay was performed as detailed in the *in vitro* method, except that the assay incubation time was 15 min and the radioligand concentration was 10 nM. A small volume of each sample homogenate was frozen on dry ice and retained for determination of drug concentration.

Measurement of drug concentrations in plasma/homogenate

Control blood and brains were obtained from rats killed by administration of CO_2. Plasma was separated from blood by centrifugation. Brain was homogenized in 50 mM Trizma buffer/0.1% BSA at pH 7.4, 4°C, using a dilution of 1 g tissue in 12 mL buffer.

Calibration lines were constructed in 2 mL 96-well polypropylene plates. Calibration lines were made using 20 μL matrix (plasma or brain homogenate) spiked with compound ranging 5–20 000 ng·mL^{-1}. Study samples were incorporated and extracted via liquid–liquid extraction (Brignol *et al.*, 2001) using pH 10 borate buffer and tert-butyl-methyl-ether. For samples that exceeded the calibration range, further dilutions in control matrix were carried out for the analysis. Extracted plates were dried under nitrogen. Samples in the extracted plates were reconstituted in 800 μL MF5 (Romil solvent; 90% water, containing 2 mM ammonium acetate and 0.027% formic acid, and 10% methanol); 10 μL was injected via a CTC-PAL autosampler on to an ultra high performance liquid chromatography-tandem mass spectrometry system. Using an Agilent 1200RR pump, a 2.1 min ballistic gradient (from 10–90% methanol/water containing 2 mM ammonium acetate and 0.027% formic acid at a flow of 1 mL·min^{-1}) was directed through a Zorbax Eclipse XDB C18 column (4.6 × 50 mm, 1.8 μm). Compound levels were detected by positive ion multiple reaction monitoring using a Turbo Ion Spray Sciex API 4000 mass spectrometer (AB SCIEX, Warrington, UK).

The free fraction (Fu) of Compound A (molecular weight 339.71) was measured via protein binding experiments. An automated equilibrium dialysis method was carried out utilizing the rapid equilibrium dialysis device (Thermo Scientific, Loughborough, UK). The prepared rapid equilibrium dialysis device was incubated on an orbital shaker for 4 h at 37°C within a humidified CO_2 chamber. Plasma and brain homogenate binding were measured individually using dialysed matrix/buffer calibration lines to quantify concentrations using ultra high performance liquid chromatography-tandem mass spectrometry. These quantified values were used for calculating protein binding. The free fraction (Fu) of Compound A in plasma and brain was calculated to be 0.425 and 0.29 respectively.

Data analysis

FLIPR assay. Data are reported as mean ± SEM of *n* experiments. Data were analysed using the non-linear regression functions within PRISM (GraphPad Software, San Diego, CA, USA).

Autoradiography. Digital images were analysed using BetaVision image analysis software (BioSpace) and binding density in a defined brain region (according to the rat brain atlas by Paxinos and Watson, 1998) was measured as digital light units per mm^2.

Homogenate binding. Data are reported as mean ± SEM of *n* experiments. Data were analysed using the non-linear regression functions within PRISM. The equilibrium dissociation constant (K_d) and the binding site density (Bmax) were derived from radioligand saturation curves using the Langmuir equation RL = RtL/(K_d + L) where L is the free ligand concentration, RL is the concentration of receptor-bound ligand at equilibrium and Rt is the total receptor concentration. IC_{50} (the concentration of compound producing 50% inhibition of specific binding) and Hill coefficients were derived from fitting to a four-parameter logistic equation. Apparent K_i values were derived using the Cheng and Prusoff equation; $K_i = IC_{50}/(1 + [L]/K_d)$ where [L] is the free concentration of radioligand and K_d is the appropriate equilibrium dissociation constant derived from the saturation analysis (Cheng and Prusoff, 1973). Apparent K_i values were converted to apparent pK_i values for illustration purposes. In kinetic experiments, the observed association rate constant (k_{obs}) and the association and dissociation half-lives were derived directly from the one-phase non-linear exponential models within PRISM. The dissociation rate constant (k_{off} in units of·$time^{-1}$) was calculated as $0.693/t_{1/2\ off}$, The association rate constant (k_{on} in units of·$time^{-1}$·nM^{-1}) was derived by the pseudo first-order method, which takes into account the concentration of radioligand used, the observed association rate constant (k_{obs} in units of·$time^{-1}$) and the dissociation rate constant (k_{off}) such that ($k_{on} = k_{obs} - k_{off}$)/[L]. The ratio of k_{off}/k_{on} was also used to estimate K_d.

For *ex vivo* receptor occupancy studies, the specific binding in each compound-treated sample was calculated as a percentage of the mean vehicle specific binding according to the following equation: (compound-treated specific binding/mean vehicle specific binding) × 100. The resulting value was then subtracted from 100% to give the percentage occupancy in the compound-treated sample.

Materials

[^{3}H]-A-804598 (2-cyano-1-[(1S)-1-phenylethyl]-3-quinolin-5-ylguanidine) was custom synthesized by GE Healthcare (UK). An extra tritium atom was incorporated to increase the specific activity from 8 Ci·$mmol^{-1}$ (Donnelly-Roberts *et al.*, 2009) to 53 Ci·$mmol^{-1}$. A-804598, Compound A (3-[1-(2-chloro-3-trifluoromethylphenyl)-1*H*-tetrazol-5-ylmethyl] pyridine hydrochloride; Nelson *et al.*, 2006) and A-740003 (*N*-(1-{[(cyanoimino)(5-quinolinyl amino) methyl]amino}-2,2-dimethylpropyl)-2-(3,4-dimethoxyphenyl)acetamide; Honore *et al.*, 2006) were synthesized at Pfizer, Sandwich, UK (chemical structures shown in Figure 1). Cell culture reagents were purchased from Invitrogen. The FLIPR Calcium 4 kit was purchased from Molecular Devices. All other supplements and chemicals were purchased from Sigma (UK).

For FLIPR assays, P2X7 antagonists were dissolved and serial dilutions prepared in 100% dimethyl sulphoxide (DMSO). The DMSO stocks were then diluted into assay buffer such that the final DMSO concentration did not exceed 1%. The equivalent concentration of DMSO was present in control wells. BZ-ATP was dissolved and diluted in assay buffer.

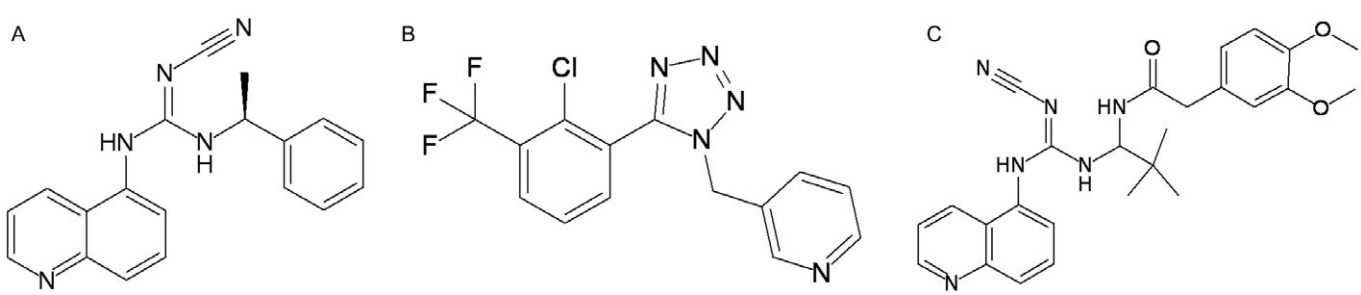

Figure 1
Chemical structure of A-804598 (A), Compound A (B) and A-740003 (C).

For *in vitro* homogenate binding, P2X7 antagonists were dissolved at 10 mM in 100% DMSO. Dilutions were made in assay buffer containing DMSO such that the % DMSO was maintained at 10% (1% in the assay). The equivalent concentration of DMSO was present in total binding wells. BZ-ATP was dissolved and diluted in assay buffer.

The drug/molecular target nomenclature in this paper conforms to the British Journal of Pharmacology Guide to Receptors and Channels (Alexander *et al.*, 2009).

Results

Functional assay

A-804598, Compound A and A-740003 produced a concentration-dependent inhibition of BZ-ATP-stimulated calcium influx with IC_{50} values (±SEM) of 28.71 ± 5.32 nM, 89.71 ± 11.39 nM and 72.27 ± 11.74 nM respectively (n = 3, Figure 2).

In vitro *autoradiography*

Autoradiographic analysis of coronal rat brain sections (Figure 3, Table 1) revealed that there was specific binding of [^{3}H]-A-804598 throughout the rat brain. The relative intensity of binding signal was colliculus >> hypothalamic nuclei (Figure 3D) = olfactory nucleus (Figure 3A) > thalamic nuclei (Figure 3D) = piriform cortex (Figure 3B) > hippocampus (Figure 3D,E) = spinal trigeminal nucleus and tract (Figure 3G) > pontine nuclei (Figure 3F) = amygdala (Figure 3D) = other cortical regions (Figure 3A–G) > cerebellum (Figure 3G) > caudate putamen (Figure 3C). High levels of [^{3}H]-A-804598 specific binding were also found in the grey matter of the L4–L6 region of the rat spinal cord.

In vitro *homogenate binding*

Specific binding of 5 nM [^{3}H]-A-804598 represented approximately 60% of total binding to rat cortex homogenate (data not shown). Specific binding of [^{3}H]-A-804598 was time-dependent, reaching a plateau after approximately 2 h, and fully reversible after the addition of an excess of A-740003 (10 μM) (Figure 4). Saturation binding confirmed that [^{3}H]-A-804598 binds with high affinity to rat cortex homogenate (Figure 5). Statistical analysis confirmed that a 1-site model was the most appropriate fit for the data obtained. Table 2 shows a summary of the binding properties of [^{3}H]-A-804598 to the rat cortex P2X7 receptor. A two sample equal variance *t*-test confirmed that there was no significant difference between the K_d value estimated from saturation analysis and the K_d obtained from the ratios of k_{off}/k_{on}

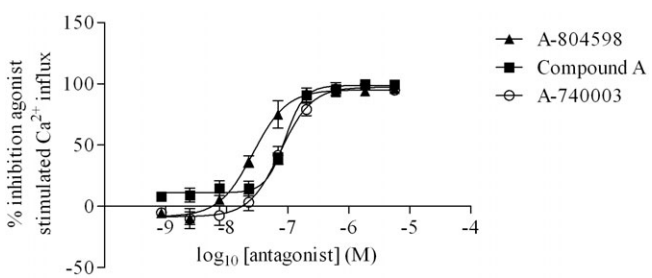

Figure 2

Effect of P2X7 antagonists on BZ-ATP (100 μM)-stimulated calcium influx in cells expressing the rat recombinant P2X7 receptor. The data are expressed as mean ± SEM (vertical lines) of three individual experiments.

Table 1

Quantification of [^{3}H]-A-804598 binding signal in rat brain and spinal cord regions

Brain region	Specific binding (cpm·mm^{-2})
Colliculus	6.96
Grey matter spinal cord	4.03
Hypothalamic nuclei	4.02
Olfactory nucleus	3.95
Thalamic nuclei	3.69
Piriform cortex	3.54
Spinal trigeminal nucleus and tract	3.29
Hippocampus	3.23
Pontine nuclei	2.96
Other cortical regions	2.93
Amygdala	2.83
Cerebellum	2.21
Caudate putamen	1.67

Table 2

Summary of binding parameters of [^{3}H]-A-804598 at the rat cortex P2X7 receptor

Parameter	Measured value
$t_{1/2}$ (on) (min)	45.12 ± 6.81
$t_{1/2}$ (off) (min)	88.24 ± 10.85
k_{off} (min^{-1})	0.0070 ± 0.0007
k_{on} (min^{-1}·nM^{-1})	0.0021 ± 0.0003
k_{off}/k_{on} (nM)	3.38 ± 0.53
K_d (nM) from saturation plot	3.08 ± 0.56
Bmax (fmol·mg^{-1})	112.90 ± 5.57

Data shown are mean ± SEM (n = 3).

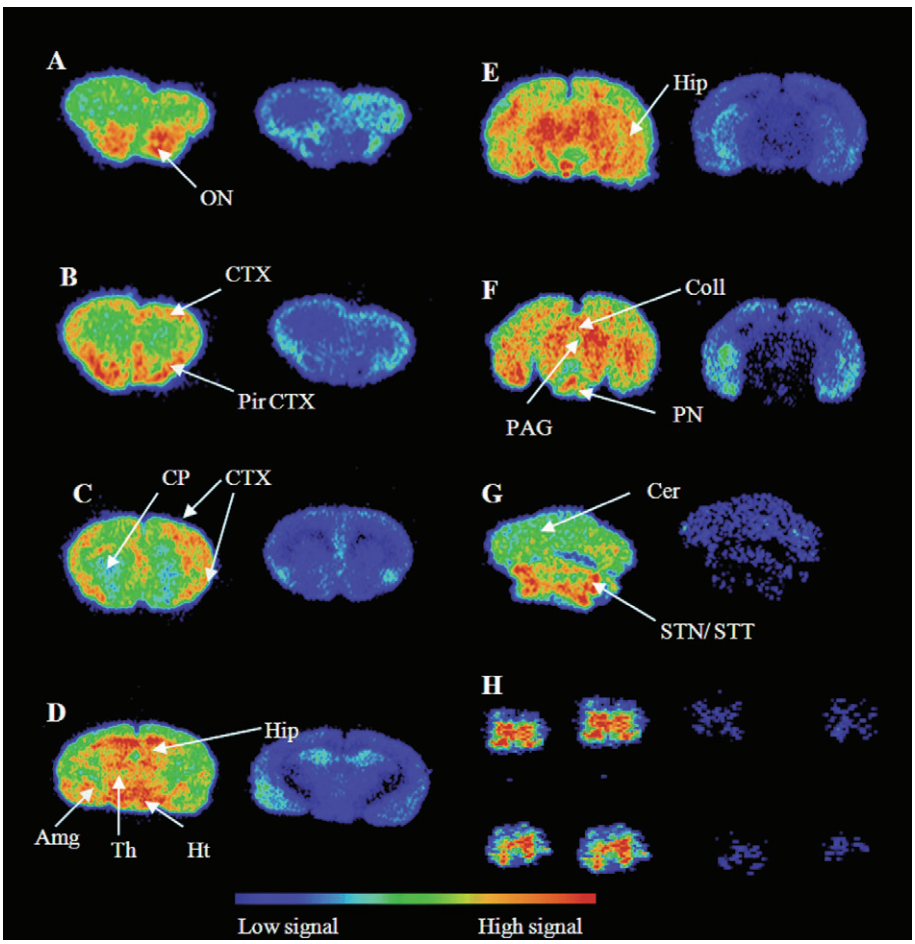

Figure 3

Localization of P2X7 receptors in coronal sections of rat brain (A–G) and spinal cord (L4–L6 region; H). For each figure, total binding sections are shown on the left, and non-specific binding sections (defined with 10 μM A-740003) are shown on the right. Amg, amygdala; Cer, cerebellum; Coll, colliculus (superior and inferior); CP, caudate putamen; CTX, cortex; Hip, hippocampus; Ht, hypothalamus; ON, olfactory nucleus; PAG, periaqueductal grey; Pir CTX, piriform cortex; PN, pontine nuclei; Th, thalamic nuclei, STN/STT, spinal trigeminal nucleus and spinal trigeminal tract.

Table 3

Apparent pK_i values for P2X7 antagonists in rat cortex binding assay

Antagonist	pK_i
A-804598	8.12 ± 0.07 (Hill slope 0.85 ± 0.09)
A-740003	7.57 ± 0.04 (Hill slope 1.49 ± 0.19)
Compound A	7.43 ± 0.03 (Hill slope 1.28 ± 0.13)
BZ-ATP	4.95 ± 0.15 (Hill slope 0.84 ± 0.13)

Data shown are means ± SEM; n = 3.

Competition experiments (Figure 6, Table 3) showed that novel P2X7 antagonists and the unlabelled form of the radioligand caused full inhibition of the specific binding of [^{3}H]-A-804598 to the rat cortex P2X7 receptor. Although Hill slopes did differ somewhat from unity, apparent K_i values were calculated to control for differences in radioactivity concentration between experiments. A-804598 was the most potent compound tested, with a K_i value of 7.51 nM. A-740003 and Compound A had K_i values of 26.51 and 37.53 nM respectively. In contrast, within the concentration range tested, BZ-ATP did not reach full inhibition and was significantly less potent, with a K_i value of 11.30 μM.

Ex vivo *receptor occupancy*

A series of optimization experiments were carried out in order to adapt the binding assay for use in *ex vivo* occupancy determination. In order to minimize the potential for drug dissociation from treated tissues, the radioligand incubation period was shortened from 2 h to 15 min. To retain an adequate specific binding signal using the reduced incubation

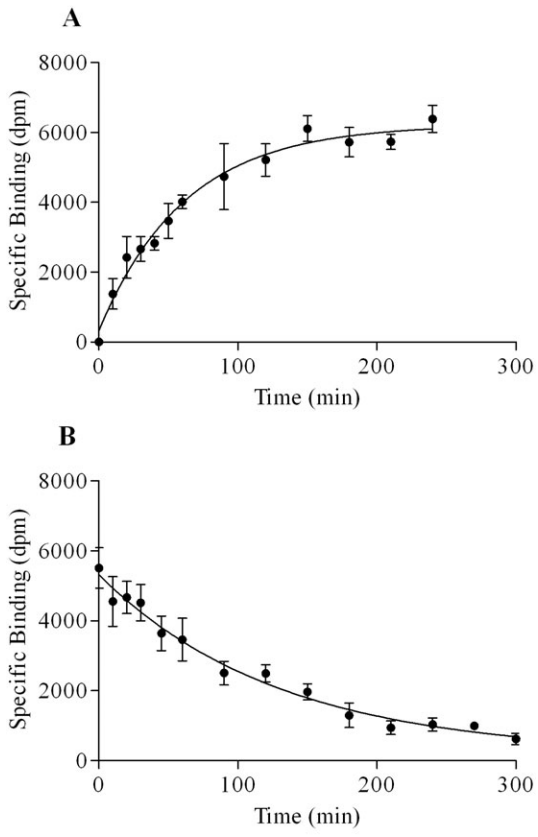

Figure 4

Binding kinetics of 5 nM [^{3}H]-A-804598 to rat cortex homogenate (300 µg protein per well). Association time-course (A) and dissociation time-course initiated by 10 µM A-740003 (B). The data are expressed as mean ± SEM (vertical lines) of three individual experiments.

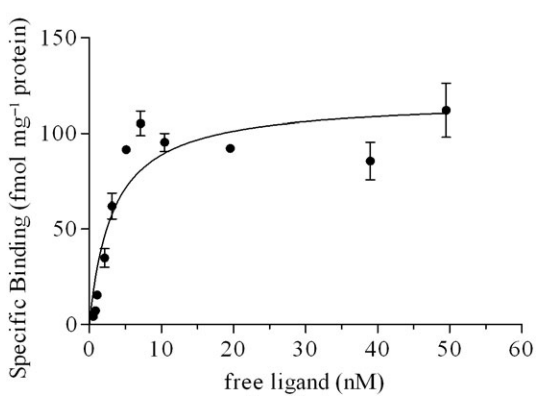

Figure 5

Saturation binding of [^{3}H]-A-804598 (0.5–50 nM) to rat cortex homogenate (300 µg protein per well). The data are expressed as mean ± SEM (vertical lines) of three individual experiments.

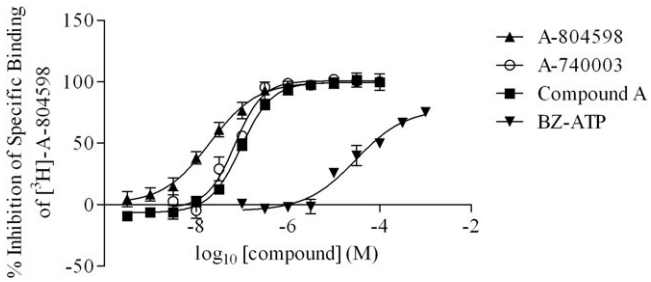

Figure 6

Competition binding of P2X7 antagonists against 5 nM [^{3}H]-A-804598 binding to rat cortex homogenate (300 µg protein per well). The data are expressed as the mean ± SEM (vertical lines) of three individual experiments.

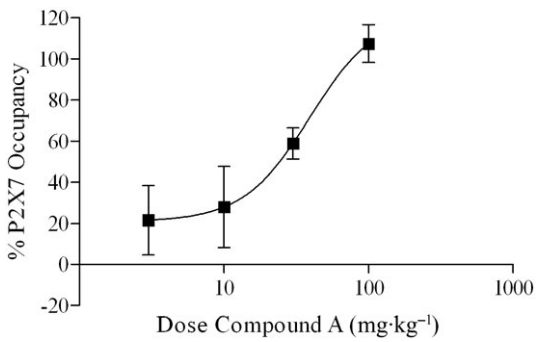

Figure 7

Ex vivo occupancy of Compound A at the P2X7 receptor in rat cortex. Data are expressed as mean ± SEM (vertical lines) of four rats per treatment group.

time, it was necessary to increase the radioligand concentration to 10 nM, and tissue protein concentration to approximately 1.75 mg per well. Under these conditions, specific binding in vehicle-treated cortex samples was maintained at 50–60%. Compound A showed dose–dependent occupancy in the rat cortex (Figure 7) with an ED_{50} value of 39.31 mg·kg^{-1}. Corresponding plasma and cortex exposure EC_{50} levels were 312.34 ng·mL^{-1} and 472.46 ng·g^{-1} respectively.

Discussion

The present study describes for the first time the autoradiographic localization of P2X7 receptors in the rat brain and spinal cord, and characterization of the binding properties of the P2X7 antagonist radioligand [^{3}H]-A-804598 in rat native tissue. Additionally, the homogenate binding methodology was successfully adapted to provide a robust *ex vivo* occupancy assay to measure target engagement of centrally penetrant P2X7 antagonists.

Before conducting radioligand binding and autoradiography experiments with [^{3}H]-A-804598, the functional potency of the unlabelled form of the radioligand, as well as that of two other novel P2X7 antagonists, was assessed using a FLIPR assay in cells expressing the rat recombinant P2X7 receptor. All three compounds potently inhibited BzATP-stimulated calcium influx, with IC_{50} values of less than 100 nM. However, A-804598 was the most potent compound tested with an IC_{50} of 28.7 nM. This is consistent with data reported by Donnelly-Roberts *et al*. (2009), who used similar methodology and generated an IC_{50} value of 9.9 nM for this compound.

Autoradiography experiments showed that binding of [^{3}H]-A-804598 was widespread throughout the rat CNS. In the literature, P2X7 has been reported to be expressed on microglia and astrocytes (Deuchars *et al*., 2001; Kukley *et al*., 2001; Xiang and Burnstock, 2005). Conflicting data exist in the literature as to the expression of the P2X7 receptor on neurones. Collo *et al*. (1997) used the techniques of *in situ* hybridization and immunohistochemistry to demonstrate the expression of P2X7 receptors on rat microglia but not neurones. Similarly, Sim *et al*. (2004) used immunohistochemistry, immunoblot and immunoprecipitation and found no evidence for the expression of the P2X7 receptor on mouse hippocampal neurones. In contrast, multiple research groups using a variety of techniques (*in situ* hybridization, immunohistochemistry, immunocytochemistry, RT-PCR) have reported data showing that P2X7 receptors are expressed on neurones (Deuchars *et al*., 2001; Armstrong *et al*., 2002; Atkinson *et al*., 2002; 2004; Lundy *et al*., 2002; Sperlágh *et al*., 2002; Ishii *et al*., 2003; Wang *et al*., 2004; Díaz-Hernandez *et al*., 2008; Marcoli *et al*., 2008).

Our autoradiography data could represent expression of the receptor on microglia, astrocytes or neurones. All cell types would be expected to be present throughout the CNS, and autoradiography does not offer sufficient resolution to determine the cellular localization of the binding of [^{3}H]-A-804598. However, it was evident that there were discrete regions where moderate-high binding intensity was observed. These include the colliculus, cerebral cortex; in particular the piriform cortex; hippocampus, hypothalamic and thalamic nuclei, amygdala, pontine nuclei, spinal trigeminal nucleus and tract, and the grey matter of the spinal cord. This is in agreement with results obtained by Yu *et al*. (2008); they recently published a study describing the use of *in situ* hybridization to demonstrate that P2X7 receptor mRNA was widely distributed throughout the rat brain. In the Yu study, the piriform cortex, hippocampus, pontine nuclei and the anterior horn of the spinal cord were among the areas of high P2X7 mRNA expression. Marcoli *et al*. (2008) demonstrated expression of P2X7 receptors on the presynaptic glutaminergic nerve terminals of rat cortical neurones. Calcium entry through these receptors was shown to evoke glutamate release, suggesting a role for the P2X7 receptor in cortical glutaminergic transmission. Wang *et al*. (2004) demonstrated the expression of P2X7 receptors on spinal cord neurones and found that inhibition of the receptor ameliorated acute spinal cord injury. Díaz-Hernandez *et al*. (2008) identified functional P2X7 receptors on the growth cones of hippocampal neurones in culture, where they appeared to play a role in neuronal growth and branching. Our data provide evidence for moderate-high expression of P2X7 in the cortex, hippocampus and spinal cord, and therefore add further support to the above findings.

The equilibrium and kinetic binding properties of [^{3}H]-A-804598 at the rat native P2X7 receptor were determined. The association half-time and K_d were consistent with those reported by Donnelly-Roberts *et al*. (2009) who investigated the binding properties of this radioligand at the rat recombinant P2X7 receptor. One discrepancy was in the dissociation half-time of the radioligand. Donnelly-Roberts *et al*. reported that the radioligand had fully dissociated from the rat recombinant P2X7 within 30 min, whereas in the present study, a dissociation half-time of 88 min was calculated. However, in the Donnelly-Roberts paper, dissociation was reported as having been conducted at room temperature as opposed to 4°C, which could account for the quicker off-rate of the radioligand.

The novel P2X7 antagonists caused full and potent inhibition of the specific binding of [^{3}H]-A-804598 to rat cortex. The standard P2X7 receptor agonist BZ-ATP had μM potency in the binding assay. This is consistent with its potency in our FLIPR assay (EC_{50} 60 μM) as well as its reported P2X7 receptor potency in diverse assay systems; for example, patch clamping experiments in rat recombinant P2X7 cells (Hibell *et al*., 2000) and ethidium bromide uptake in rat peritoneal cells (Chen *et al*., 2005).

In the *ex vivo* occupancy assay, Compound A showed dose–dependent occupancy at the cortex P2X7 receptor, reaching maximal occupancy at 100 mg·kg^{-1}. It is anticipated that the current *ex vivo* occupancy data may provide confidence for demonstrating target engagement using positron emission tomography imaging in clinical studies.

In summary, a P2X7 receptor radioligand binding assay in rat native tissue has been reported for the first time. Specific binding of [^{3}H]-A-804598

was shown to be of high affinity, saturable and reversible in rat cortex homogenate. Novel P2X7 antagonists inhibited specific binding of the radioligand to rat cortex with affinities consistent with their functional potency at the rat recombinant P2X7 receptor. The radioligand can also be used to measure *ex vivo* occupancy of P2X7 antagonists in rat cortex, which could provide an important biomarker in pre-clinical studies. Given the therapeutic potential for compounds that bind to the P2X7 receptor, a native tissue P2X7 receptor binding and occupancy assay could form an important component of a drug discovery programme.

Acknowledgement

The authors wish to thank Kevin Dack for chemistry expertise.

Conflict of interest

The authors state no conflict of interest.

References

Alexander SPH, Mathie A, Peters JA (2009). Guide to receptors and channels (GRAC). Br J Pharmacol 158 (Suppl. 1): S1–S254.

Anderson CM, Nedergaard M (2006). Emerging challenges of assigning P2X7 receptor function and immunoreactivity in neurons. Trends Neurosci 29: 257–262.

Armstrong JN, Brust TB, Lewis RG, MacVicar BA (2002). Activation of presynaptic P2X7-like receptors depresses mossy fiber–CA3 synaptic transmission through p38 Mitogen-Activated Protein Kinase. J Neurosci 22: 5938–5945.

Atkinson L, Milligan CJ, Buckley NJ, Deuchars J (2002). An ATP-gated ion channel at the cell nucleus. Nature 420: 42.

Atkinson L, Batten TF, Moores TS, Varoqui H, Erickson JD, Deuchars J (2004). Differential co-localisation of the P2X7 receptor subunit with vesicular glutamate transporters VGLUT1 and VGLUT2 in rat CNS. Neuroscience 123: 761–768.

Bianco F, Ceruti S, Colombo A, Fumagalli M, Ferrari D, Pizzirani C *et al*. (2006). A role for P2X7 in microglial proliferation. J Neurochem 99: 745–758.

Brignol N, McMahon LM, Luo S, Tse FL (2001). High-throughput semi-automated 96-well liquid/liquid extraction and liquid chromatography/mass spectrometric analysis of everolimus (RAD 001) and cyclosporin a (CsA) in whole blood. Rapid Commun Mass Spectrom 15: 898–907.

Bulanova E, Budagian V, Orinska Z, Hein M, Petersen F, Thon L *et al*. (2005). Extracellular ATP induces cytokine expression and apoptosis through P2X7 receptor in murine mast cells. J Immunol 174: 3880–3890.

Chen Y-W, Donnelly-Roberts DL, Namovic MT, Gintant GA, Cox BF, Jarvis MF *et al*. (2005). Pharmacological characterization of P2X7 receptors in rat peritoneal cells. Inflamm Res 54: 119–126.

Cheng Y, Prusoff WH (1973). Relationship between the inhibition constant (Ki) and the concentration of inhibitor which causes 50 percent inhibition (IC50) of an enzymatic reaction. Biochem Pharmacol 22: 3099–3108.

Chessell IP, Simon J, Hibell AD, Michel AD, Barnard EA, Humphrey PP (1998). Cloning and functional characterisation of the mouse P2X7 receptor. FEBS Lett 439: 26–30.

Collo G, Neidhart S, Kawashima E, Kosco-Vilbois M, North RA, Buell G (1997). Tissue distribution of the P2X7 receptor. Neuropharmacology 36: 1277–1283.

Deuchars SA, Atkinson L, Brooke RE, Musa H, Milligan CJ, Batten TF *et al*. (2001). Neuronal P2X7 receptors are targeted to presynaptic terminals in the central and peripheral nervous systems. J Neurosci 21: 7143–7152.

Díaz-Hernandez M, del Puerto A, Díaz-Hernandez JI, Diez-Zaera M, Lucas JJ, Garrido JJ *et al*. (2008). Inhibition of the ATP-gated P2X7 receptor promotes axonal growth and branching in cultured hippocampal neurons. J Cell Sci 121: 3717–3728.

Donnelly-Roberts DL, Namovic MT, Surber B, Vaidyanathan SX, Perez-Medrano A, Wang Y *et al*. (2009). [3H]A-804598 ([3H]2-cyano-1-[(1S)-1-phenylethyl]-3-quinolin-5-ylguanidine) is a novel, potent, and selective antagonist radioligand for P2X7 receptors. Neuropharmacology 56: 223–229.

Ferrari D, Villalba M, Chiozzi P, Falzoni S, Ricciardi-Castagnoli P, Di Virgilio F (1996). Mouse microglial cells express a plasma membrane pore gated by extracellular ATP. J Immunol 156: 1531–1539.

Ferrari D, Chiozzi P, Falzoni S, Dal Susino M, Melchiorri L, Baricordi OR *et al*. (1997). Extracellular ATP triggers IL-1 beta release by activating the purinergic P2Z receptor of human macrophages. J Immunol 159: 1451–1458.

Hibell AD, Kidd EJ, Chessell IP, Humphrey PP, Michel AD (2000). Apparent species differences in the kinetic properties of P2X7 receptors. Br J Pharmacol 130: 167–173.

Honore P, Donnelly-Roberts D, Namovic MT, Hsieh G, Zhu CZ, Mikusa JP *et al*. (2006). A-740003 [*N*-(1-{[(cyanoimino)(5-quinolinylamino) methyl]amino}-2,2-dimethylpropyl)-2-(3,4-dimethoxyphenyl)acetamide], a

novel and selective P2X7 receptor antagonist, dose-dependently reduces neuropathic pain in the rat. J Pharmacol Exp Ther 319: 1376–1385.

Ishii K, Kaneda M, Li H, Rockland KS, Hashikawa T (2003). Neuron-specific distribution of P2X7 purinergic receptors in the monkey retina. J Comp Neurol 459: 267–277.

Kukley M, Barden JA, Steinhauser C, Jabs R (2001). Distribution of P2X receptors on astrocytes in juvenile rat hippocampus. Glia 36: 11–21.

Lundy PM, Hamilton MG, Mi L, Gong W, Vair C, Sawyer TW *et al*. (2002). Stimulation of Ca2+ influx through ATP receptors on rat brain synaptosomes: identification of functional P2X7 receptor subtypes. Br J Pharmacol 135: 1616–1626.

Marcoli M, Cervetto C, Paluzzi P, Guarnieri S, Alloisio S, Thellung S *et al*. (2008). $P2X_7$ presynaptic receptors in adult rat cerebrocortical nerve terminals: a role in ATP-induced glutamate release. J Neurochem 105: 2330–2342.

Nelson DW, Gregg RJ, Kort ME, Perez-Medrano A, Voight EA, Wang Y *et al*. (2006). Structure-activity relationship studies on a series of novel, substituted 1-benzyl-5-phenyltetrazole P2X7 antagonists. J Med Chem 49: 3659–3666.

Nicke A, Kuan Y-H, Masin M, Rettinger J, Marquez-Klaka B, Bender O *et al*. (2009). A functional P2X7 splice variant with an alternative transmembrane domain 1 escapes gene inactivation in P2X7 KO mice. J Biol Chem 284: 25813–25822.

North RA (2002). Molecular physiology of P2X receptors. Physiol Rev 82: 1013–1067.

Paxinos G, Watson C (1998). *The Rat Brain in Stereotaxic Coordinates, Fourth Edition*. Academic Press: San Diego, CA.

Rassendren F, Buell GN, Virginio C, Collo G, North RA, Surprenant A (1997). The permeabilising ATP receptor, P2X7. Cloning and expression of a human cDNA. J Biol Chem 272: 5482–5486.

Sim JA, Young MT, Sung HY, North RA, Surprenant A (2004). Reanalysis of P2X7 receptor expression in rodent brain. J Neurosci 24: 6307–6314.

Sperlágh B, Hasko G, Nemeth Z, Vizi ES (1998). ATP released by LPS increases nitric oxide production in raw 264.7 macrophage cell line via P2Z/P2X7 receptors. Neurochem Int 33: 209–215.

Sperlágh B, Köfalvi A, Deuchars J, Atkinson L, Milligan CJ, Buckley NJ *et al*. (2002). Involvement of P2X7 receptors in the regulation of neurotransmitter release in the rat hippocampus. J Neurochem 81: 1196–1211.

Suadicani SO, Brosnan CF, Scemes E (2006). P2X7 receptors mediate ATP release and amplification of astrocytic intercellular Ca2+ signalling. J Neurosci 26: 1378–1385.

Surprenant A, Rassendren F, Kawashima E, North RA, Buell G (1996). The cytolytic P2Z receptor for extracellular ATP identified as a P2X receptor (P2X7). Science 272: 735–738.

Wang X, Arcuino G, Takano T, Lin J, Peng WG, Wan P *et al*. (2004). P2X7 receptor inhibition improves recovery after spinal cord injury. Nat Med 10: 821–827.

Xiang Z, Burnstock G (2005). Expression of P2X receptors on rat microglial cells during early development. Glia 52: 119–126.

Yu Y, Ugawa S, Ueda T, Ishide Y, Inoue K, Nyunt AK *et al*. (2008). Cellular localization of P2X7 receptor mRNA in the rat brain. Brain Res 1194: 45–55.